Applied Catalysis B: Environmental 166–167 (2015) 37–44

Contents lists available at ScienceDirect

Applied Catalysis B: Environmental

journal homepage: www.elsevier.com/locate/apcatb

The role of ceria on the activity and SO_2 resistance of catalysts for the selective catalytic reduction of NOx by NH_3

Dong Wook Kwon, Ki Bok Nam, Sung Chang Hong*

Department of Environmental Energy Engineering, Graduate School of Kyonggi University, 94-6 San, Iui-dong, Youngtong-ku, Suwon-si, Gyeonggi-do 443-760, Republic of Korea

ARTICLE INFO

Article history:
Received 29 July 2014
Received in revised form 31 October 2014
Accepted 3 November 2014
Available online 13 November 2014

Keywords:
Ceria effect
SO_2 resistance
NH_3-SCR
V/Sb/Ce/Ti
CeO_2

ABSTRACT

We investigated the influence of Ce on the catalytic activity of V/Sb/Ce/Ti and its deactivation due to SO_2. We studied the properties of the catalyst using physio-chemical techniques, including transmission infrared spectroscopy (IR), NH_3 and SO_2 temperature programmed desorption (TPD), X-ray photoelectron spectroscopy (XPS), H_2 temperature programmed reduction (H_2-TPR), and thermal gravimetric analysis (TGA). The catalysts V/Sb/Ti and V/Sb/Ce/Ti showed an excellent NOx conversion and N_2 selectivity in the temperature range of 200–400 °C. Increasing Brønsted acid sites and the NH_3 adsorption positively affected the efficiency of the catalyst. The Ce^{4+} ratio increased upon the addition of Sb and V to Ce/Ti. The catalyst V/Sb/Ce/Ti was prepared by controlling the Ce^{4+} ratio and exhibited an excellent activity upon increasing the Ce^{4+} ratio. The V/Sb/Ti (or V/W/Ti) showed one route in which NH_4HSO_4 formed by converting SO_2 into SO_3 upon the injection of SO_2 in the selective catalytic reduction (SCR) reaction. In addition to this route, the reaction in the presence of V/Sb/Ce/Ti can proceed via a second route, in which $Ce_2(SO_4)_3$ is formed in the reaction of Ce with SO_2 and O_2. Thus, V/Sb/Ce/Ti can inhibit the formation of NH_4HSO_4 due to the consumption of SO_2 in the formation of $Ce_2(SO_4)_3$. Therefore, V/Sb/Ce/Ti was found to have excellent SO_2 resistance compared to V/Sb/Ti (or V/W/Ti).

1. Introduction

Nitrogen oxides (NOx) are a major air pollutant. They are primarily emitted during the combustion of fossil fuels from stationary and mobile sources [1–3]. It is well known that the selective catalytic reduction (SCR) of NOx with NH_3 is a superior technology for the removal of NOx in terms of removal efficiency, stability, and costs. In this process, NOx contained in the fuel gases is reduced to N_2 and H_2O by NH_3 [4]:

$$4NO + 4NH_3 + O_2 \rightarrow 4N_2 + 6H_2O \quad (1)$$

Various studies on the development of SCR catalysts have been conducted in order to improve their activities, e.g. through the addition of metals. For example, the support [5], V_2O_5-MnOx-TiO_2 [6], and different alkali and alkaline earth metals (Na, K, Ca, and Mg) have been used to supplement V_2O_5-WO_3/TiO_2 [7], F-doped V_2O_5-WO_3/TiO_2 [8], and Cr-V_2O_5/TiO_2 [9]. In particular, a recent study demonstrated high NOx conversion rates at low temperatures using ceria (CeO_2) as co-catalyst [10–13]. Ceria has been extensively studied regarding its redox properties and its exceptional ability to store and release oxygen via the redox shift between Ce^{4+} and Ce^{3+} under oxidizing or reducing conditions, respectively [14]. Ceria accelerates the oxidization of NO to NO_2 and the SCR of NO to N_2 by ammonia [15].

Most fossil fuels contain sulfur, and the exhaust gas contains a substantial amount of sulfur dioxide (SO_2). According to some reports, SO_2 forms sulfate species on the catalyst surface and enhances the SCR activity. Guo et al. claimed that an excellent NO reduction activity was observed since the density of Brønsted acid sites increases upon the sulfation of V_2O_5/TiO_2 [16]. According to Amiridis et al. [17], the turnover frequency was increased under conditions of a low vanadium surface coverage if the surface of the sulfate species was formed on the V_2O_5 catalyst. In addition, SO_2 poisons the NH_3-SCR catalyst at low temperatures since sulfur compounds can form at the catalyst in the presence of SO_2. Various studies have been performed to inhibit the degradation of vanadium-titanium-based catalysts by SO_2. Kobayashi et al. [18,19] confirmed that the oxidation rate of SO_2 decelerates as the SiO_2 concentration increases, provided the SiO_2 concentrations in V_2O_5/SiO_2-TiO_2 and V_2O_5/SiO_2-TiO_2-MoO_3 were below 20 wt%. Seo et al. [20] reported that the milling process enhanced non-stoichiometric oxide concentrations (V^{x+} ($x \leq 4$) and Ti^{y+} ($y \leq 3$))

* Corresponding author. Tel.: +82 31 249 9733; fax: +82 31 254 4941.
E-mail addresses: schong@kgu.ac.kr, schong@kyonggi.ac.kr (S.C. Hong).

http://dx.doi.org/10.1016/j.apcatb.2014.11.004
0926-3373/

as well as the redox capacity of the V_2O_5/TiO_2 catalyst. In addition, it was reported that the formation of ammonium sulfate salts was inhibited. Liu et al. [21] claimed that the SCR activity and the H_2O/SO_2 durability were excellent since the surface of $FeVO_4/TiO_2$ was enriched with VO_x species that acted as the true active sites. According to Ha et al. [22], Sb at 2 wt% showed a better SO_2 resistance than tungsten at 10 wt% because of its high electrical conductivity. Wu et al. [23] reported an increased efficiency and SO_2 resistance at 150 °C due to the addition of ceria to Mn/TiO_2. Lee et al. [24] claimed that the SO_2 adsorption decreased and SO_2 resistance increased by the addition of ceria to the SbV/TiO_2 catalyst. Thus far, many studies have been conducted to examine the efficiency of the NH_3-SCR catalyst and the promotion of SO_2 resistance.

Among these studies, experiments showing an improved activity and SO_2 resistance due to the addition of Sb and Ce provide very interesting results. Therefore, on the basis of the above literature, we aim to investigate the role of Ce in the catalyst V/Sb/Ce/Ti. We studied the correlation between the catalysts Ce valence state and its activity. In addition, we clearly identified the cause of the increased SO_2 resistance by deactivating the catalyst with the addition of Ce. We studied the properties of the catalyst using physio-chemical analyses, which included transmission infrared (IR) spectroscopy, NH_3 and SO_2 temperature programmed desorption (TPD), X-ray photoelectron spectroscopy (XPS), H_2 temperature programmed reduction (H_2-TPR), and thermal gravimetric analysis (TGA).

2. Experiments

2.1. Catalyst preparation

V/Ce/Ti and V/Sb/Ce/Ti were prepared by the wet impregnation of vanadium (2 wt% V) and antimony (2 wt% Sb) on a prepared Ce/Ti support. V/Sb/Ti was prepared by wet impregnation of vanadium and antimony on a prepared Ti support. V/W/Ti was prepared by wet impregnation of vanadium and tungsten (5 wt% W) on a prepared Ti support. The required quantity of ammonium metavanadate (NH_4VO_3, Aldrich Chemical Co.) was added to an oxalic acid ($(COOH)_2$, Aldrich Chemical Co.) solution and heated to form an ammonium oxalate solution. An aqueous solution of antimony was prepared using antimony acetate ($Sb(CH_3COO)_3$, Alfa Aesar). Ammonium metatungstate hydrate ($(NH_4)_6H_2W_{12}O_{40}$, Aldrich Co.) was used as W precursor. Both of these solutions were added to the beaker containing the calculated amount of the Ce/Ti powder; TiO_2 was combined with this solution by gradual stirring. This mixed solution, which was in a slurry state, was then stirred for more than an hour. Subsequently, the water was evaporated at 70 °C using a rotary vacuum evaporator (Eyela Co. N-N series). Then, the samples were dried for an additional 24 h at 103 °C in a dry oven to remove residual water. The samples were then calcined in air for 4 h at 500 °C. The Ce/Ti support was synthesized by a deposition precipitation method followed by the hydrolysis with ammonium hydroxide (Aldrich, 25%) [25]. Therefore, the required quantities of cerium(III) nitrate (10 wt% Ce; $Ce(NO_3)_3{\cdot}6H_2O$, Aldrich Chemical Co.) and commercial TiO_2 (DT-51, Cristal Global Co.) powders were mixed in water. To this solution, dilute aqueous ammonia was added as a precipitating agent, and the resultant precipitate was filtered. The sample was dried for an additional 24 h at 103 °C in a dry oven to remove residual water. Then, the sample was calcined in air for 4 h at 500 °C [24]. The x in V/Sb/Ce/Ti(x) is denoted as follows: x = the calcination temperature of the Ce/Ti support at 400, 450, 500, 550, and 600 °C. V/Sb/Ce/Ti(x) were prepared using commercial TiO_2 (G-5, Cristal Global Co. G-5 was used as titanic acid, which was in this state prior to the final calcination step upon the manufacture of anatase TiO_2).

2.2. Catalytic activity tests

SCR activity tests were carried out in a fixed-bed quartz-reactor with an inner diameter of 8 mm. The reactant gases were fed to the reactor using a mass flow controller (MKS Co.). The reaction conditions were as follows: 750 ppm NO, 48 ppm NO_2, 800 ppm NH_3, 3 vol% O_2, 6 vol% H_2O, and 500 ppm SO_2 in Ar. Approximately, 0.3 g of the catalyst (40–50 mesh, 0.6 cm^3) was used for each test. Under ambient conditions, the total flow rate was 600 cm^3/min and the gas hourly space velocity was 60,000 h^{-1}. The composition of the feed gases and the effluent streams were continuously monitored on-line using non-dispersive infrared gas analyzers: ZKJ-2 (Fuji Electric Co.) for NO/NO_2, and Ultramat 6 (Siemens Co.) for N_2O, and the pulsed fluorescence gas analyzer 43 C-High level (Thermo Co.) for SO_2. Before the gas flowed into the analyzers, the moisture was removed with a moisture trap inside the chiller. The NOx conversion and rate constant were calculated from the concentrations of the gases at steady state according to the following equations:

$$NO_x \text{ conversion}\,(\%) = \frac{([NO + NO_2]_{in} - [NO + NO_2]_{out})}{[NO + NO_2]_{in}} \times 100 \quad (2)$$

$$N_2 \text{ selectivity}\,(\%) = \frac{(([NO]_{in} + [NH_3]_{in}) - [NO_2]_{out} - 2[N_2O]_{out})}{([NO]_{in} + [NH_3]_{in})} \times 100 \quad (3)$$

$$NH_3 \text{ conversion}\,(\%) = \frac{[NH_3]_{in} - [NH_3]_{out}}{[NH_3]_{in}} \times 100 \quad (4)$$

2.3. Catalyst characterizations

In situ DRIFTs analysis was used in this study and performed with an FT-IR 660 Plus (JASCO Co.). A DR (Diffuse Reflectance) 400 accessory was used for solid reflectance analysis. The CaF_2 window was used as a plate for DR measurement; spectra were collected using a mercury cadmium telluride (MCT) detector. All of the catalysts used in the analysis were ground using a rod in the sample pan of an in situ chamber with an installed temperature controller. To exclude the influence of moisture and impurities, the sample was preprocessed with Ar at a rate of 100 cm^3/min at 300 °C for 1 h; then, the vacuum state was maintained using a vacuum pump. To collect the spectra of the catalyst, a single-beam spectrum of the preprocessed sample was measured as background, and all analyses were performed through auto scanning at a resolution of 4 cm^{-1}.

NH_3 temperature programmed desorption measurements were carried out with 0.3 g samples of the catalysts under a total flow rate of 50 cm^3/min. Before the TPD measurements, the catalysts were pretreated in a flow of 5% O_2/Ar at 300 °C for 0.5 h and subsequently cooled to 50 °C. The samples were then treated with 1% NH_3/Ar for 1 h. The NH_3 was purged with Ar for 2 h before starting the TPD experiments. During the TPD experiments, the quantity of NH_3 (m/e 15) was continuously monitored using a quadrupole mass spectrometer (QMS 422) while the temperature was increased to 600 °C at a rate of 10 °C/min.

An ESCALAB 210 (VG Scientific) was used for X-ray photoelectron spectroscopy (XPS) analysis with monochromatic Al Kα (1486.6 eV) as the excitation source. After the complete removal of moisture from the catalysts by drying at 100 °C for 24 h, the analysis was performed without surface sputtering and etching, so that the degree of vacuum in the XPS equipment was maintained at 10^{-6} Pa. Spectra were analyzed using the XPS PEAK software (version 4.1). The intensities were estimated from the integration of each peak, subtraction of the Shirley background, and fitting of the experimental curve to a combination of Lorentzian and Gaussian curves of various proportions. All binding energies were referenced to the C 1s line at 284.6 eV. Binding energy values were measured with a precision of ±0.3 eV.

The temperature programmed reduction (TPR) of H_2 was measured using 10% H_2/Ar and 0.3 g of the catalyst at a total flow rate

of 50 cm^3/min. Before the H_2-TPR measurement, the catalyst was pretreated in a flow of 5% O_2/Ar at 400 °C for 0.5 h, followed by cooling to 50 °C. The catalyst was placed in dilute hydrogen and the consumption of hydrogen was monitored with Autochem 2920 (Micrometrics) by increasing the temperature to 600 °C at a rate of 10 °C/min.

SO_2 temperature programmed desorption measurements were carried out with 0.3 g samples of the catalysts with a total flow rate of 50 cm^3/min. Before the TPD measurements, the catalysts were pretreated in a flow of 5% O_2/Ar at 300 °C for 0.5 h and then cooled to 250 °C. The samples were then treated with 1% SO_2/Ar for 1 h. The SO_2 was purged with Ar for 2 h before starting the TPD experiments. During the TPD experiments, the quantity of SO_2 (m/e 64) was continuously monitored using a quadrupole mass spectrometer (QMS 422) while the temperature was increased to 900 °C at a rate of 10 °C/min.

TGA experiments were conducted by a thermo gravimetric analyzer (TGA) from TA Instruments. The catalyst was loaded into the TGA reactor, and the reactor was purged with N_2 for 5 min. The temperature of the TGA furnace was increased to 120 °C and kept constant for 20 min to remove adsorbed water. The temperature was then increased to 900 °C at a rate of 10 °C/min under N_2 atmosphere.

The transmission IR spectra were recorded with a Nicolet Nexus spectrometer (Model Magna IR 550 II) equipped with a liquid nitrogen cooled MCT detector, which collected 100 scans with a spectral resolution of 4 cm^{-1}. The samples were mixed with KBr and pressed into pellets for the measurements.

3. Results and discussion

3.1. NH_3-SCR catalyst activity

The experiments were performed using vanadium-titanium-based catalysts to examine the influence of antimony and ceria on the selective catalytic reduction activity. As shown in Fig. 1(a), the NOx conversion activity was determined on Ce/Ti, V/Ce/Ti, V/Sb/Ti, V/Sb/Ce/Ti, and V/W/Ti at 200–400 °C with a GHSV of 60,000 h^{-1}. The Ce/Ti exhibited an activity below 70% at temperatures up to 300 °C. V/Ce/Ti prepared by impregnating vanadium on the Ce/Ti support showed a higher efficiency compared with Ce/Ti at temperatures up to 300 °C. However, since large amounts of N_2O (30 ppm) were produced due to the oxidation of NH_3, which was injected as a reducing agent at approximately 270 °C, this catalyst showed the lowest N_2 selectivity. V/Sb/Ti and V/Sb/Ce/Ti showed an excellent N_2 selectivity and activity in the range of 250–400 °C. N_2 selectivity and activity were enhanced at 200–400 °C as Sb was added to V/Ce/Ti. In the case of V/W/Ti, the activity was similar to that of V/Sb/Ti and V/Sb/Ce/Ti at 250 °C or higher. However, it showed a slightly lower activity at temperatures up to 200 °C. Fig. 1(b) shows the NH_3 conversion for the SCR reaction. This conversion is proportional to the NOx conversion since the SCR reaction is held at a molar ratio of 1.0 NH_3/NOx. Therefore, the NH_3 conversion curve was associated with the temperature range in which the NOx conversion decreased.

3.2. NH_3 adsorption study

The catalytic activity of Ce/Ti, V/Ce/Ti, V/Sb/Ti, and V/Sb/Ce/Ti varied depending on the metal impregnated on the titanium support. To investigate the reason for this, the NH_3 adsorption capacity of various catalysts was compared. The adsorption ability of the catalysts was measured by DRIFTs and NH_3-TPD analysis.

To examine the acid site of the catalysts in the SCR reaction, a NH_3 adsorption analysis was performed using a DRIFT

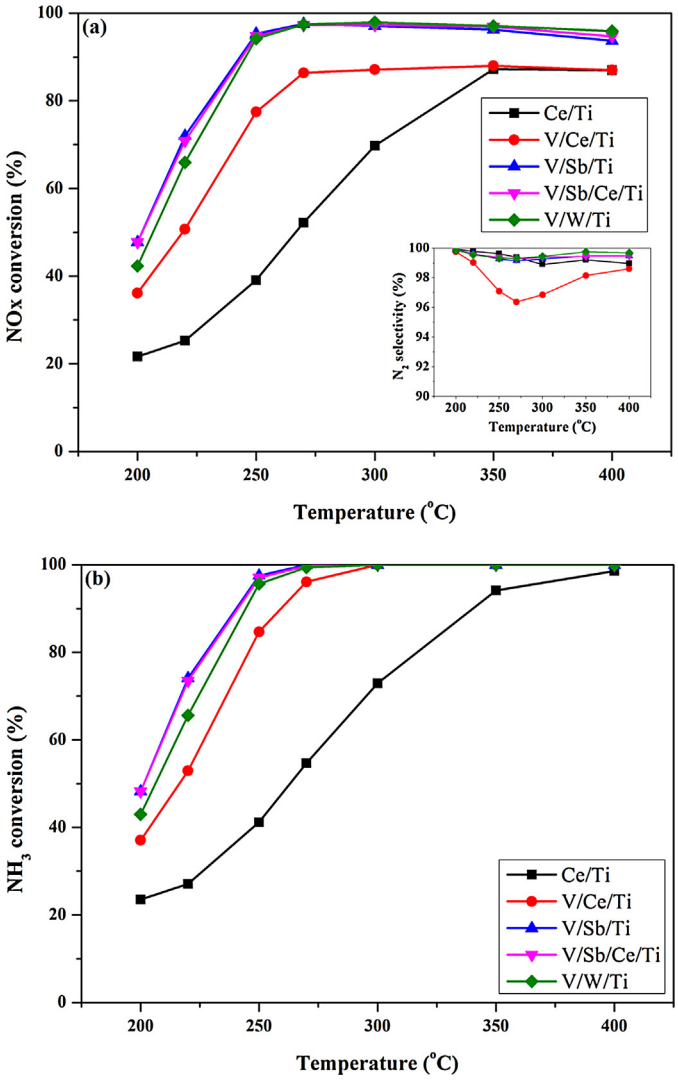

Fig. 1. The effect of reaction temperature on (a) NOx conversion and (b) NH_3 conversion of various catalysts (NO: 750 ppm, NO_2: 48 ppm, NH_3/NOx: 1.0, O_2: 3 vol%, H_2O: 6 vol%, S.V.: 60,000 h^{-1}).

spectrometer at 250 °C. These measurements showed a clear difference in the activity (Fig. 2). NH_3 (2000 ppm) was injected for 30 min and the adsorbed species were examined. In these experiments, the peak corresponding to –OH, caused by the adsorption of NH^{4+} onto –OH, was observed at 3644 cm^{-1}. The adsorption of NH_3 on the Lewis acid sites was observed at 1605, 3170, 3256, and 3364 cm^{-1} [26]. All catalysts exhibited peaks corresponding to Lewis acid sites and –OH. In the case of V/Ce/Ti, V-Sb/Ti, and V/Sb/Ce/Ti impregnated with vanadium, a negative peak was observed at 2040 cm^{-1}, which corresponds to V=O [27]. Additionally, the adsorption of the NH^{4+} ion on the Brønsted acid sites was simultaneously observed at 1430 and 1670 cm^{-1} [26]. In the case of Ce/Ti, the Brønsted acid sites showed a very small peak. In the case of Ce/Ti impregnated vanadium, it seemed that the Brønsted acid sites were more abundant compared with those on Ce/Ti. Additionally, the number of Brønsted acid sites was increased by the addition of Sb to V/Ce/Ti. V/Sb/Ti and V/Sb/Ce/Ti revealed the largest peaks corresponding to Brønsted acid sites and showed an excellent catalytic activity at 250 °C. In addition, the largest negative peak of the adsorption of NH^{4+} onto —OH was observed at 3644 cm^{-1} for V/Sb/Ti and V/Sb/Ce/Ti. At 250 °C, where the difference in catalytic activity was clearly distinguished, the activity tended to increase concomitantly with the peak corresponding to NH^{4+} adsorbed

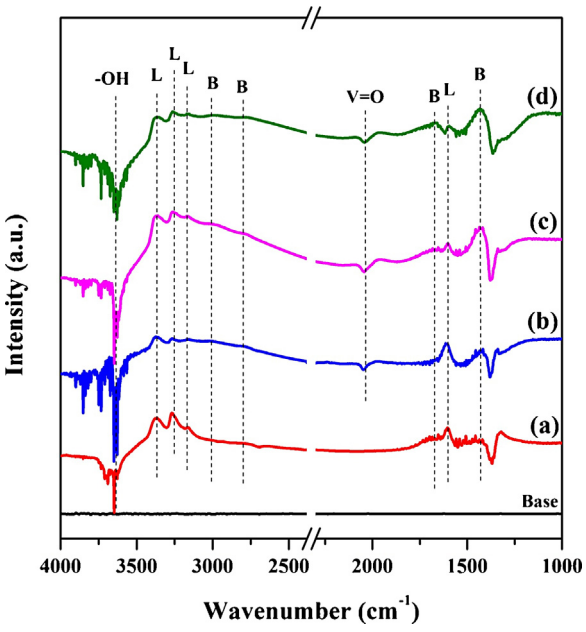

Fig. 2. DRIFT spectra of (a) Ce/Ti, (b) V/Ce/Ti, (c) V/Sb/Ti and (d) V/Sb/Ce/Ti exposed to 2000 ppm NH_3 for 30 min at 250 °C.

on the Brønsted acid sites. The intensities for the Brønsted acid site peaks decreased in the order V/Sb/Ce/Ti (12.3) ≈ V/Sb/Ti (12.2) > V/Ce/Ti (6.0) > Ce/Ti (1.0) (the ratio of the deconvoluted Brønsted acid site peak areas in DRIFTs). This suggests that NH^{4+} adsorbs on the Brønsted acid sites, which correlates strongly with the catalytic activity as also shown in previous studies [28–30].

To further determine the effect of the NH_3 adsorption on the SCR, NH_3-TPD was measured after saturation of the catalysts with NH_3. Fig. 3 shows the NH_3-TPD curves of various catalysts. All of the catalysts exhibited two broad NH_3 desorption peaks at 80–200 and 230–400 °C, which were attributed to the Brønsted and Lewis acid sites, respectively. It is well known that ammonia desorbs from Brønsted acid sites at lower temperatures than it desorbs from Lewis acid sites [31,32]. The desorption peak in the temperature range of 80–500 °C was the largest when V/Sb/Ce/Ti was employed. The peak areas of NH_3-TPD decreased in the order V/Sb/Ce/Ti (1.00) > V/Sb/Ti (0.81) > V/Ce/Ti (0.70) > Ce/Ti (0.67). The Brønsted acid sites increased with an increasing catalytic activity, but the total acidity showed different results. V/Sb/Ce/Ti showed a large

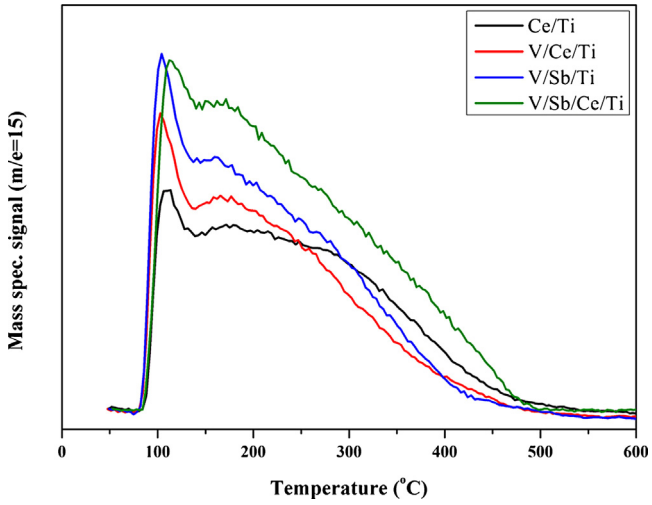

Fig. 3. NH_3-TPD patterns of Ce/Ti, V/Ce/Ti, V/Sb/Ti and V/Sb/Ce/Ti.

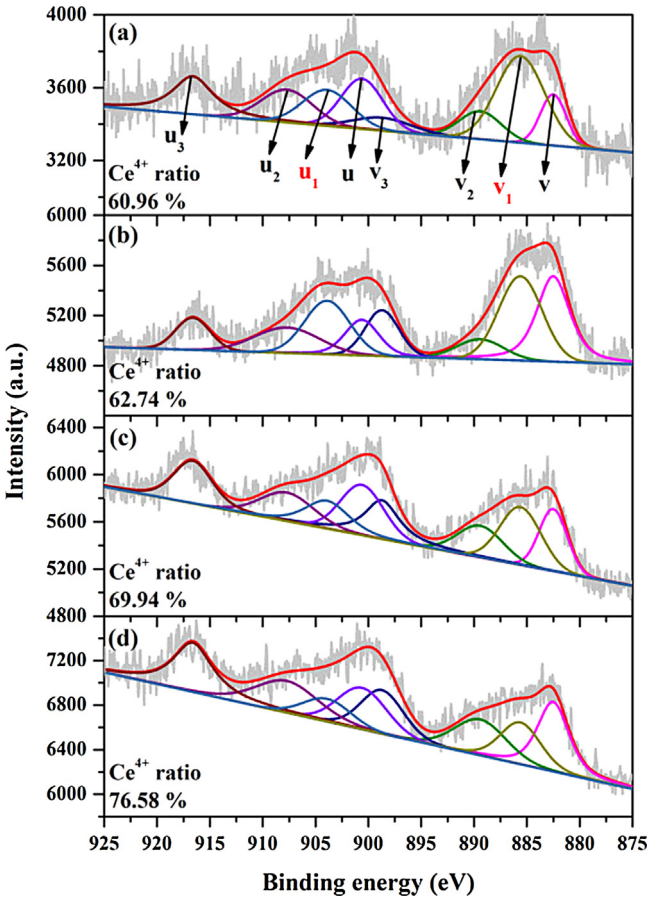

Fig. 4. Ce 3d spectra of (a) Ce/Ti, (b) V/Ce/Ti, (c) V/Sb/Ti and (d) V/Sb/Ce/Ti by XPS analysis.

amount of NH_3 desorption peaks corresponding to Lewis acid sites at temperatures of 200 °C or higher. The total acidity of V/Sb/Ce/Ti increased more than that of V/Sb/Ti. These findings suggest an increase in the Lewis acid sites, which is ascribed to the addition of ceria. As revealed by the catalytic activity of Ce/Ti, ceria could be applied as an active metal in SCR catalysis [33–36] and could harbor NH_3 adsorption capacity. V/Sb/Ce/Ti had a higher NH_3 adsorption capacity than V/Sb/Ti owing to the addition of ceria. When ceria was added to V/Sb/Ti, the total acidity increased due to the increase in Lewis acid sites, whereas the catalytic activity remained constant.

3.3. Ce valence state study

The valence state of the involved metals is an important factor in the SCR reaction, which for Ce was either Ce^{4+} or Ce^{3+}. Thus, the valence states of Ce were examined in Ce/Ti, V/Ce/Ti, and V/Sb/Ce/Ti with various activities. In addition, the Ce valence state of Sb/Ce/Ti without the impregnation of vanadium was examined in V/Sb/Ce/Ti. Fig. 4 shows the XPS peaks of Ce 3d for Ce/Ti, Sb/Ce/Ti, V/Ce/Ti, and V/Sb/Ce/Ti. The Ce 3d peak was fitted into sub-bands by searching for the optimum combination of Gaussian bands. The sub-bands labeled u_1 and v_1 represent the $3d^{10}4f^1$ initial electronic state corresponding to Ce^{3+}. The sub-bands labeled u, u_2, u_3, v, v_2, and v_3 represent the $3d^{10}4f^0$ state of Ce^{4+} [11]. The Ce^{4+} ratios of all samples were calculated by $Ce^{4+}/(Ce^{3+} + Ce^{4+})$. The Ce^{4+} ratios decreased in the order of V/Sb/Ce/Ti (76.85%) > V/Ce/Ti (69.94%) > Sb/Ce/Ti (62.74%) > Ce/Ti (60.96%). The Ce^{4+} ratio of Ce/Ti was 60.96% and it gradually increased with the impregnation of Sb, Ce, and Sb/Ce. Table 1 shows the catalyst activities and the Ce^{4+} ratios for Ce/Ti, V/Ce/Ti, and V/Sb/Ce/Ti. As Sb and/or Ce were

Table 1
The ratio of deconvoluted Brønsted acid site peak areas in DRIFTs, Ce^{4+} ratio of catalysts and their activities. The following conditions were employed: 750 ppm NO, 48 ppm NO_2, 1.0 NH_3/NOx, 3% O_2, 6% H_2O, S.V. 60,000 h^{-1}.

Catalyst	The ratio of Brønsted acid site	Ce^{4+} ratio (%)	NOx conversion at 250 °C (%)	NOx conversion at 200 °C (%)
Ce/Ti	1.0	60.96	38.86	21.41
V/Ce/Ti	6.0	69.94	77.48	36.14
V/Sb/Ce/Ti	12.3	76.58	94.80	47.77

added to Ce/Ti, the ratio of the Brønsted acid sites increased. Thus, an excellent activity resulted and the Ce^{4+} ratio increased as well. Changes of the Ce valence state were observed upon addition of the metal to Ce/Ti. When CeO_2 was added to TiO_2, ceria interacted with Ce and Ti and formed the valence states Ce^{4+} and Ce^{3+} (Ce^{4+}: 60.96%). When Sb or V was added, an oxygen bridge of Ce–O–Sb or Ce–O–V was formed by the stable V_2O_5 (or Sb_2O_5), which increased the amount of ceria and the oxygen binding. When both Sb and V were simultaneously added to Ce/Ti, the amount of Ce–O–Sb(V) oxygen bridges increased as well as the Ce^{4+} ratio. These findings indicate that the elements Ce^{4+}, Sb, and V supported on TiO_2 exert a positive synergetic interaction and accelerate the SCR reaction. Yang et al. [37] clarified how the presence of Ce^{4+} on the catalyst surface enhances the SCR reaction. They reported that Ce^{4+} activated adsorbed NH_3 on the surface to form NH_2, which then reacts with gaseous NO to form N_2 and H_2O.

The dependence of the catalytic activity on the Ce valence state was examined on V/Sb/Ce/Ti. Lee et al. [38] reported that the Ce^{4+}/Ce^{3+} ratio varied depending on the temperature of the thermal treatment of Ce/Ti during the catalyst preparation. In this study, V and Sb were impregnated after the thermal treatment temperature of Ce/Ti was changed and V/Sb/Ce/Ti was prepared. To thoroughly investigate the thermal treatment effects of ceria and TiO_2, TiO_2 was used as titanic acid, which is the state prior to the final calcination step upon the manufacture of anatase TiO_2. Fig. 5 shows the Ce 3d XPS peak of V/Sb/Ce/Ti(400–600). The Ce^{4+} ratios varied for all catalysts prepared at the thermal treatment temperature of Ce/Ti. The Ce^{4+} ratios in V/Sb/Ce/Ti(400–600) decreased in the order of V/Sb/Ce/Ti(500) > V/Sb/Ce/Ti(550) > V/Sb/Ce/Ti(600) > V/Sb/Ce/Ti(450) > V/Sb/Ce/Ti(400). The highest Ce^{4+} ratio was obtained when the thermal treatment of Ce/Ti was performed at a temperature of 500 °C. Fig. 6 shows the correlation of the Ce^{4+} ratio and the catalytic activity. The Ce^{4+} ratio of V/Sb/Ce/Ti(500) was 82.48%. An increase in the Ce^{4+} ratio resulted in an excellent catalytic activity.

H_2-TPR analysis was carried out to investigate the presence of reducible species in V/Sb/Ce/Ti(400–600). To distinguish the vanadium and antimony peaks in V/Sb/Ce/Ti(400–600), H_2-TPR analyses of V/Ti and V/Sb/Ti were performed. Fig. 7 shows the results of the H_2-TPR analysis for V/Ti, V/Sb/Ti, and V/Sb/Ce/Ti(400–600). All catalysts exhibited major reduction peaks at temperatures in the range of 300–550 °C. Both peaks were observed at 380 and 403 °C in V/Ti. According to a previous study, the high temperature reduction peak is generally attributed to the reduction of vanadium in polymeric and bulk-like V_2O_5 species. The low temperature reduction peak is ascribed to highly dispersed vanadium species or monomeric species [39–41]. A new peak at a temperature of 426 °C was observed for the V-Sb/Ti catalyst. Since SbOx species were reduced at a higher temperature than VOx species [42], the peak at 426 °C could possibly be caused by Sb. Upon the addition of ceria, V/Sb/Ce/Ti(400–600) exhibited peaks other than V/Ti and V/Sb/Ti at higher temperature. According to the literature [15], the TPR peak at approximately 480 °C could be ascribed to the surface reduction of Ce^{4+} to Ce^{3+}. The XPS Ce 3d spectra (Fig. 5) reveal that the peak at 480 °C increased in V/Sb/Ce/Ti(500) with the highest amount of Ce^{4+}. Thus, a higher Ce^{4+} ratio was beneficial for the catalytic efficiency of V/Sb/Ce/Ti and occurred when the thermal treatment temperature of Ce/Ti was 500 °C.

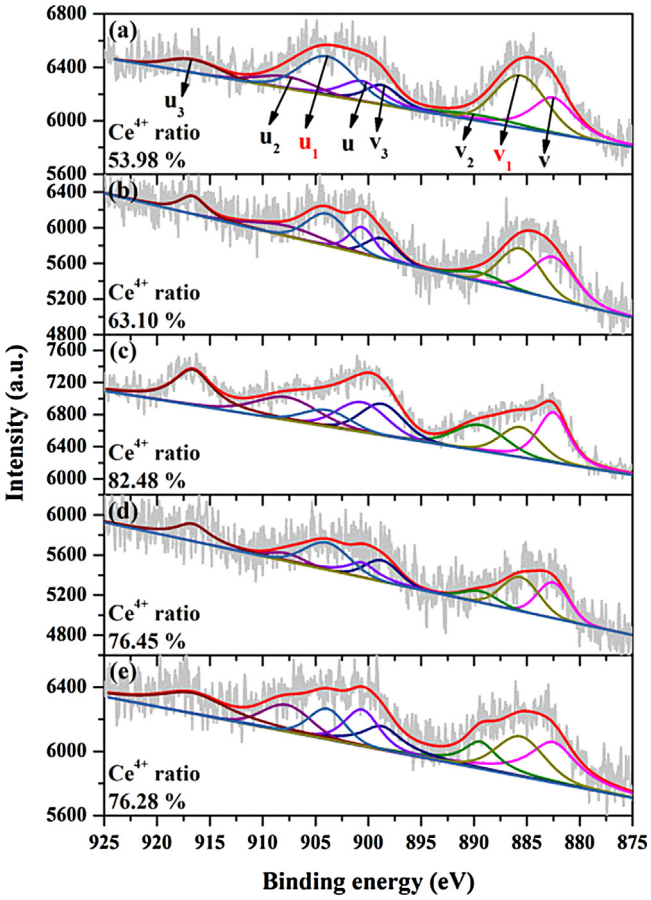

Fig. 5. Ce 3d spectra of (a) V/Sb/Ce/Ti(400), (b) V/Sb/Ce/Ti(450), (c) V/Sb/Ce/Ti(500), (d) V/Sb/Ce/Ti(550) and (e) V/Sb/Ce/Ti(600) by XPS analysis.

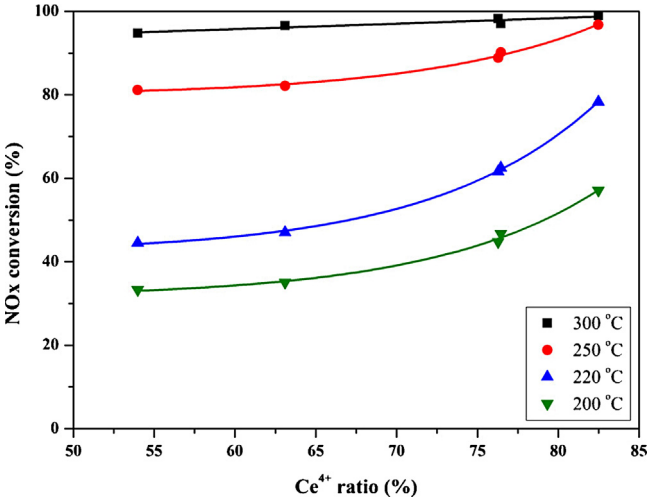

Fig. 6. Correlation of the Ce^{4+} ratio with NOx conversion over V/Sb/Ce/Ti(*x*00).

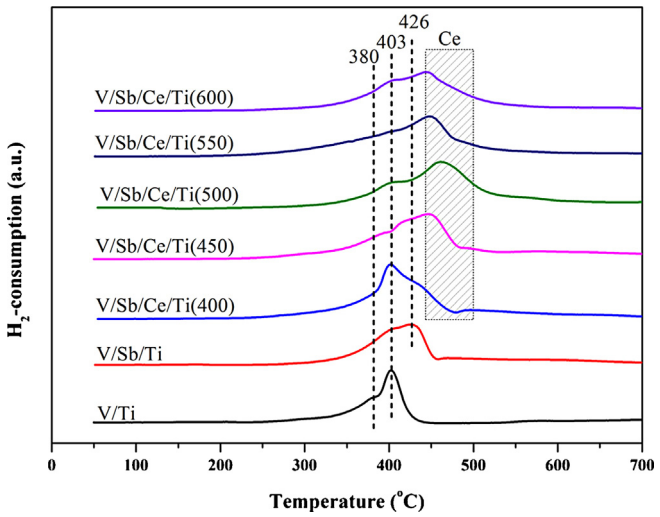

Fig. 7. H_2-TPR profiles of V/Ti, V/Sb/Ti and V/Sb/Ce/Ti(x00) (experimental conditions: 30 mg cat, pretreatment at 400 °C for 30 min with 5% O_2/Ar 50 cm^3/min, 10% H_2/Ar reduction with heating rate 10 °C/min, total flow rate 50 cm^3/min).

3.4. SO_2 resistance study

The effects of SO_2 addition on the activity of V/Sb/Ti, V/Sb/Ce/Ti, and V/W/Ti were monitored as a function of time on stream during the SCR of NO by NH_3. The reaction conditions were as follows: 750 ppm NO, 48 ppm NO_2, NH_3/NOx = 1.0, 3 vol% O_2, 6 vol% H_2O, 500 ppm SO_2, S.V. = 60,000 h^{-1}, and a total flow rate of 600 cm^3/min at 250 °C. The activities of all catalysts were detected until they decreased to 0.85 with respect to their initial activities. Fig. 8(a) depicts the time dependence of the relative catalytic activity (k/k_0) on the proceeding SO_2 reaction, initiated by the addition of SO_2 at t = 0.0 h. The initial efficiency was found to be more than 96% for all catalysts. The activity gradually decreased depending on the SO_2 injection time. V/W/Ti and V/Sb/Ti showed a rapid deactivation upon the addition of SO_2 in comparison with V/Sb/Ce/Ti. The duration times of V/W/Ti and V/Sb/Ti were 24.5 and 32.5 h at the final k/k_0 ratio of 0.85. In comparison to this, V/Sb/Ce/Ti exhibited a very high duration time of 58 h at a k/k_0 ratio of 0.85. The mechanisms of the SO_2 oxidation and sulfation reactions on the catalyst surface had been clarified as follows [43]: (1) (V^{3+})-SO_3(ads) formed when SO_2(g) coordinated to the terminal oxygen V=O; (2) (V^{3+})-SO_3(ads) converted to SO_3(g); (3) SO_3(g) induced the deactivation of the catalyst by forming NH_4HSO_4, which resulted from the reaction of NH_3 and H_2O. It is well known that the deactivation of V_2O_5/TiO_2 in the presence of SO_2 at low temperatures is primarily due to the blocking of the catalyst pores caused by the formation of NH_4HSO_4, which SO_3 oxidizes more readily than supported V_2O_5, NH_3, and H_2O [9,44]. For all catalysts, a similar drop in NH_3, approximately 20 ppm, during the SCR reaction was detected in the absence of SO_2. The difference in the deactivation of V/W/Ti, V/Sb/Ti, and V/Sb/Ce/Ti in the presence of SO_2 is possibly caused by the reaction between the catalysts and SO_2 rather than with NH_3. The time dependence of catalyst deactivation due to SO_2 was studied by detecting the outlet SO_2 concentration, as shown in Fig. 8(b). The outlet SO_2 concentration started to decrease at the same point of time as the catalytic activity. The decrease in NH_3 results from a decrease in the catalytic activity and is accelerated by deactivation of the catalyst, which is caused by the reaction with SO_2. The outlet SO_2 concentration was measured initially for 1 h after the injection of SO_2 into V/Sb/Ti, V/Sb/Ce/Ti, and V/W/Ti (Fig. 8(c)). V/W/Ti exhibited a low SO_2 resistance after reacting for 1 h with the highest concentration of SO_2. Separately, V/Sb/Ce/Ti exhibited an excellent SO_2 resistance after reacting with the lowest concentrations of SO_2.

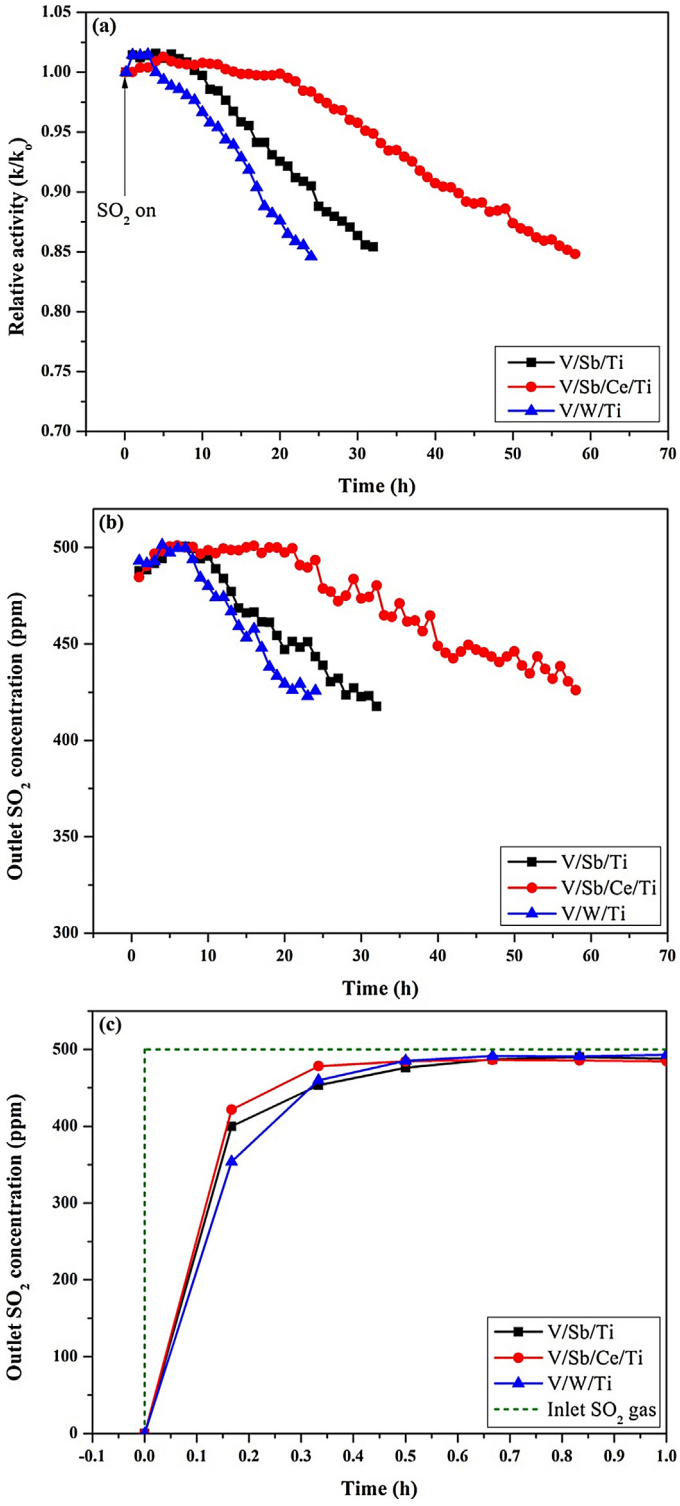

Fig. 8. (a) Relative activity, (b) outlet SO_2 concentration, (c) outlet SO_2 concentration (for the initial 1 h) in the presence of SO_2 for the SCR of NO by NH_3 over V/Sb/Ti, V/Sb/Ce/Ti and V/W/Ti at 250 °C (NO: 750 ppm, NO_2: 48 ppm, NH_3/NOx: 1.0, O_2: 3 vol%, H_2O: 6 vol%, SO_2: 500 ppm, S.V.: 60,000 h^{-1}).

In addition, changes in catalytic activity with respect to the initial catalytic activity were observed upon SO_2 injection. SCR activities of V/Sb/Ti, V/Sb/Ce/Ti, and V/W/Ti were determined after 20 h deactivation with SO_2 (Fig. 9). V/Sb/Ce/Ti, which had an excellent SO_2 resistance, exhibited an activity similar to its initial activity, but the activities of V/Sb/Ti and V/W/Ti were lower. Thus, V/Sb/Ce/Ti showed a better SO_2 resistance than V/Sb/Ti and V/W/Ti.

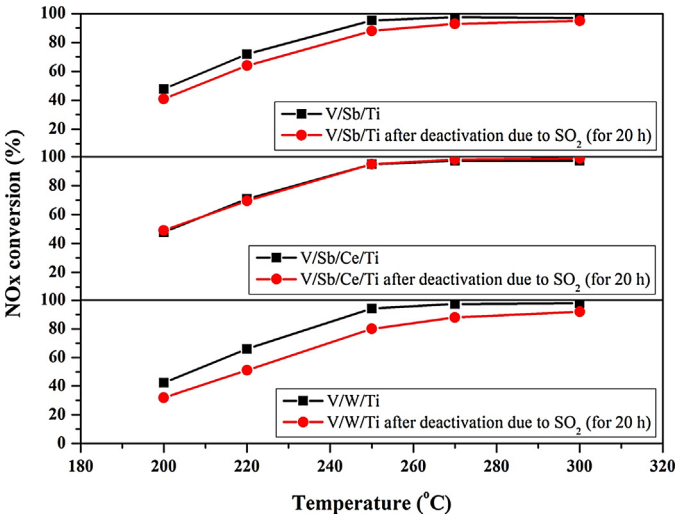

Fig. 9. The effect of reaction temperature on NOx conversion of V/Sb/Ti, V/Sb/Ce/Ti and V/W/Ti after deactivation due to SO_2 for 20 h (NO: 750 ppm, NO_2: 48 ppm, NH_3/NOx: 1.0, O_2: 3 vol%, H_2O: 6 vol%, S.V.: 60,000 h^{-1}).

To clarify the deactivation due to SO_2, we examined the SO_2-TPD for V/W/Ti, V/Sb/Ti, and V/Sb/Ce/Ti after exposure to 5000 ppm SO_2 for 1 h at 250 °C. Fig. 10 shows the dependence of the SO_2 (64 m/z) signals on the temperature, which exhibits one peak and one shoulder peak around 610 and 700 °C, respectively, for V/W/T, and two peaks around 615 and 700 °C for V/Sb/Ti. The low-temperature peak might be assigned to the desorption of SO_2 adsorbed to the catalyst surface. The high-temperature peak might originate from an impurity or from the desorption of SO_2 adsorbed to the catalyst in the bulk [45]. This peak appeared around 770 °C for V/Sb/Ti. In addition, for the SO_2-TPD of Ce/Ti, the peak at 700–875 °C corresponds to a sulfated ceria species. This study considered that CeO_2 formed the species $Ce_2(SO_4)_3$ by the reaction with SO_2 using the catalyst V/Sb/Ce/Ti. The SO_2-TPD measurements reveal that SO_2 rapidly decreases the deactivation efficiency of V/W/Ti and its desorption spectrum shows the largest peak. The SO_2-TPD peak of V/Sb/Ti decreased than V/W/Ti. This indicates that the addition of antimony inhibits the reaction of the vanadium and SO_2. The SO_2-TPD of V/Sb/Ce/Ti showed that the addition of antimony and ceria inhibited the reaction of vanadium and SO_2 more efficiently by reducing the amount of adsorbed SO_2. The peak of V/Sb/Ce/Ti at 770 °C is related to the formation of $Ce_2(SO_4)_3$ from SO_2 and

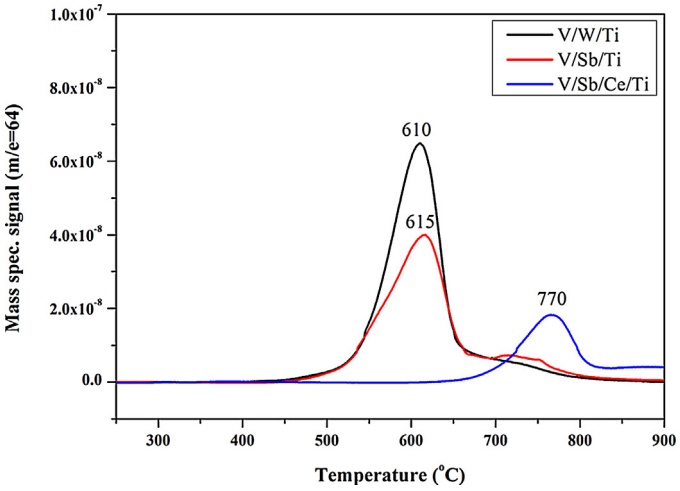

Fig. 10. SO_2-TPD patterns of V/W/Ti, V/Sb/Ti and V/Sb/Ce/Ti.

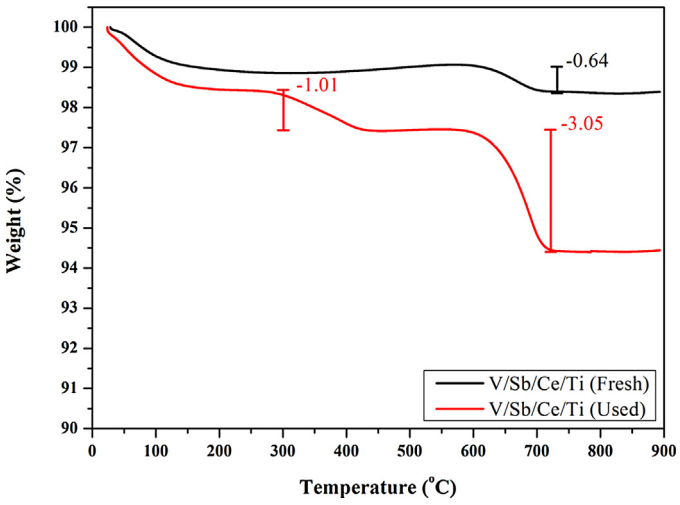

Fig. 11. TGA curves of V/Sb/Ce/Ti (fresh) and V/Sb/Ce/Ti (used) samples.

was extremely decreased in intensity. The SO_2-TPD peak decreased due to the deactivation of the catalyst upon SO_2 adsorption. This result demonstrates the excellent resistance of V/Sb/Ce/Ti against the deactivation due to SO_2.

The resistance to SO_2 greatly improved during the SO_2 deactivation experiment when ceria was added to V/Sb/Ce/Ti in comparison with V/Sb/Ti. To identify the cause, thermal gravimetric analysis (TGA) and transmission infrared spectroscopy (IR) of fresh and used samples were performed of V/Sb/Ce/Ti. The TGA spectra (Fig. 11) reveal a loss of mass of the used sample in two steps in the temperature ranges of 270–435 and 600–720 °C. The cause of the decrease in catalytic activity was the formation of ammonium sulfate on the catalyst surface during the deactivation due to SO_2. The loss of mass at 270–435 °C was caused by the decomposition of $(NH_4)_2SO_4$ [46], while the loss of mass at 600–720 °C corresponds to $Ce_2(SO_4)_3$. Fresh and used samples showed weight reductions of 0.64 wt% and 3.05 wt%, respectively. The amount of $Ce_2(SO_4)_3$ increased as CeO_2 reacted with SO_2 and O_2 during the progress of the experiment.

Fig. 12 shows the transmission IR spectra of the fresh and used catalysts. For the used sample, several bands at 982, 1196, 1128, 1414, and 1631 cm^{-1}, and a wide band at 3400–3500 cm^{-1} were detected. According to the literature [47], the strong bands at 1196

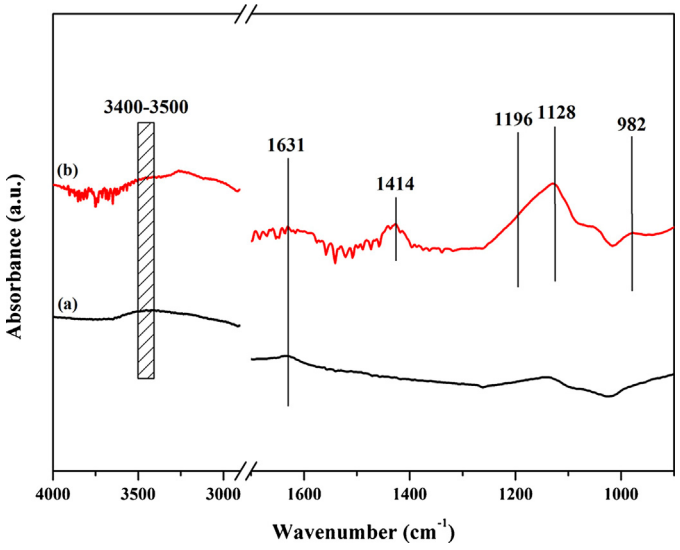

Fig. 12. Transmission IR spectra of (a) V/Sb/Ce/Ti (fresh) and (b) V/Sb/Ce/Ti (used) samples.

and 1128 cm^{-1} are caused by bulk sulfate on the CeO_2 catalyst. The bands at 982 and 1414 cm^{-1} are due to surface sulfate species with only one S=O double bond, and three S–O bonds with the O atoms linked to the surface. The broad bands between 3400 and 3500 cm^{-1} and the band at 1631 cm^{-1} were assigned to H_2O [48]. It can be concluded that both surface and bulk sulfate species formed on the used sample. The bulk sulfate species correspond to $Ce_2(SO_4)_3$, which decomposes at high temperature.

In summary, the catalyst V/Sb/Ce/Ti had a better SO_2 resistance compared with that of V/Sb/Ti (or V/W/Ti). In the case of V/Sb/Ti (or V/W/Ti), the deactivation progressed since SO_2 was oxidized to SO_3 after the injection, which induced the formation of NH_4HSO_4 on the surface of the catalyst. In the case of V/Sb/Ce/Ti, other reactions proceed upon SO_2 injection in addition to the formation of NH_4HSO_4. SO_2 formed $Ce_2(SO_4)_3$ by reacting with CeO_2 and H_2O. Since SO_2 was consumed in the formation of $Ce_2(SO_4)_3$, the oxidization of SO_2 to SO_3 substantially decreased compared with V/Sb/Ti (or V/W/Ti). Thus, the addition of Ce had a positive effect on delaying the catalyst deactivation in the presence of SO_2.

4. Conclusions

We investigated the effects of Ce on the activity and the deactivation due to SO_2 of the catalyst V/Sb/Ce/Ti. In V/Sb/Ti and V/Sb/Ce/Ti, Brønsted acid sites developed and similar activities were shown. The Ce^{4+} ratio increased upon the addition of Sb and V to Ce/Ti. V/Sb/Ce/Ti was prepared by adjusting the Ce^{4+} ratio and showed an excellent activity when the Ce^{4+} ratio was increased. V/Sb/Ti (or V/W/Ti) formed NH_4HSO_4 by the conversion of SO_2 to SO_3 by performing the SCR reaction in the presence of SO_2 (one route). However, V/Sb/Ce/Ti shows additional reactions upon the injection of SO_2, aside from the reaction that forms NH_4HSO_4. At V/Sb/Ce/Ti, CeO_2 forms $Ce_2(SO_4)_3$ by reacting with SO_2 and O_2 (two routes). V/Sb/Ce/Ti suppresses the production of NH_4HSO_4 since the injected SO_2 is consumed upon the formation of $Ce_2(SO_4)_3$. V/Sb/Ce/Ti shows an excellent SO_2 resistance compared with that of V/Sb/Ti (or V/W/Ti). In other words, CeO_2 formed cerium sulfate on the surface of V/Sb/Ce/Ti in the reaction with SO_2 and O_2. SO_2 poisons the catalyst, and once it is converted to cerium sulfate, the formation of ammonium bi-sulfate is suppressed.

References

[1] G. Qi, R.T. Yang, J. Catal. 217 (2003) 434–441.
[2] P.S. Metkar, M.P. Harold, V. Balakotaiah, Appl. Catal. B: Environ. 111–112 (2012) 67–80.
[3] S. Roy, M.S. Hedge, G. Madras, Appl. Energy 86 (2009) 2283–2297.
[4] P. Forzatti, Appl. Catal. A: Gen. 222 (2001) 221–236.
[5] Y. Zhang, X. Zhu, K. Shen, H. Xu, K. Sun, C. Zhou, J. Colloid Interface Sci. 376 (2012) 233–238.
[6] X. Wu, Z. Si, G. Li, D. Weng, Z. Ma, J. Rare Earths 29 (2011) 64–68.
[7] L. Chen, J. Li, M. Ge, Chem. Eng. J. 170 (2011) 531–537.
[8] S. Zhang, H. Li, Q. Zhong, Appl. Catal. A: Gen. 435–436 (2012) 156–162.
[9] H. Huang, L. Jin, H. Lu, H. Yu, Y. Chen, Catal. Commun. 34 (2013) 1–4.
[10] L. Chen, J. Li, M. Ge, Environ. Sci. Technol. 44 (2010) 9590–9596.
[11] W. Shan, F. Liu, H. He, X. Shi, C. Zhang, Appl. Catal. B: Environ. 115–116 (2012) 100–106.
[12] W. Shana, F. Liu, H. He, X. Shi, C. Zhang, Catal. Today 184 (2012) 160–165.
[13] H. Chang, J. Li, J. Yuan, L. Chen, Y. Dai, H. Arandiyan, J. Xu, J. Hao, Catal. Today 201 (2013) 139–144.
[14] B.M. Reddy, A. Khan, Y. Yamada, T. Kobayashi, S. Loridant, J.C. Volta, J. Phys. Chem. B 107 (2003) 5162–5167.
[15] L. Chen, J. Li, M. Ge, J. Phys. Chem. C 113 (2009) 21177–21184.
[16] X. Guo, C. Bartholomew, W. Hecker, L.L. Baxter, Appl. Catal. B: Environ. 92 (2009) 30–40.
[17] M.D. Amiridis, I.E. Wachs, G. Deo, J.M. Jehng, D.S. Kim, J. Catal. 161 (1996) 247–253.
[18] M. Kobayashi, R. Kuma, A. Morita, Catal. Lett. 112 (2006) 37–44.
[19] M. Kobayashi, R. Kuma, S. Masaki, N. Sugishima, Appl. Catal. B: Environ. 60 (2005) 173–179.
[20] P.W. Seo, J.Y. Lee, K.S. Shim, S.H. Hong, S.C. Hong, S.I. Hong, J. Hazard. Mater. 165 (2009) 39–47.
[21] F. Liu, H. He, Z. Lian, W. Shan, L. Xie, K. Asakura, W. Yang, H. Deng, J. Catal. 307 (2013) 340–351.
[22] H.H. Phil, M.P. Reddy, P.A. Kumar, L.K. Ju, J.S. Hyo, Appl. Catal. B: Environ. 78 (2008) 301–308.
[23] Z. Wu, R. Jin, H. Wang, Y. Liu, Catal. Commun. 10 (2009) 935–939.
[24] K.J. Lee, P.A. Kumar, M.S. Maqbool, K.N. Rao, K.H. Song, H.P. Ha, Appl. Catal. B: Environ. 142–143 (2013) 705–717.
[25] K.N. Rao, B.M. Reddy, S.E. Park, Appl. Catal. B: Environ. 100 (2010) 472–480.
[26] N.Y. Topsoe, J.A. Dumesic, H. Topsoe, J. Catal. 151 (1995) 241–252.
[27] N.Y. Topsoe, H. Topsoe, J.A. Dumesic, J. Catal. 151 (1995) 226–240.
[28] F. Tang, B. Xu, H. Shi, J. Qiu, Y. Fan, Appl. Catal. B: Environ. 94 (2010) 71–76.
[29] Y. Zheng, A.D. Jensen, J.E. Johnsson, Ind. Eng. Chem. Res. 43 (2004) 941–947.
[30] D. Nicosia, I. Czekaj, O. Kröcher, Appl. Catal. B: Environ. 77 (2008) 228–236.
[31] J.G. Amores, V.S. Escribano, G. Ramis, G. Busca, Appl. Catal. B: Environ. 13 (1997) 45–58.
[32] G. Busca, L. Lietti, G. Ramis, F. Berti, Appl. Catal. B: Environ. 18 (1998) 1–36.
[33] W. Xu, Y. Yu, C. Zhang, H. He, Catal. Commun. 9 (2008) 1453–1457.
[34] X. Gao, Y. Jiang, Y. Fu, Y. Zhong, Z. Luo, K. Cen, Catal. Commun. 11 (2010) 465–469.
[35] L. Chen, J. Li, M. Ge, R. Zhu, Catal. Today 153 (2010) 77–83.
[36] W. Shan, F. Liu, H. He, X. Shi, C. Zhang, ChemCatChem 3 (2011) 1286–1289.
[37] S. Yang, Y. Guo, H. Chang, L. Ma, Y. Peng, Z. Qu, N. Yan, C. Wang, J. Li, Appl. Catal. B: Environ. 136–137 (2013) 19–28.
[38] S.M. Lee, H.H. Lee, S.C. Hong, Appl. Catal. A: Gen. 470 (2014) 189–198.
[39] D.W. Kwon, K.H. Park, S.C. Hong, Appl. Catal. A: Gen. 451 (2013) 227–235.
[40] I. Giakoumelou, C. Fountzoula, C. Kordulis, S. Boghosian, J. Catal. 239 (2006) 1–12.
[41] G. Du, S. Lim, M. Pinault, C. Wang, F. Fang, L. Pfefferle, G.L. Haller, J. Catal. 253 (2008) 74–90.
[42] H. Zhang, Z. Liu, Z. Feng, C. Li, J. Catal. 260 (2008) 295–304.
[43] J.P. Dunn, P.R. Koppula, H.G. Stenger, I.E. Wachs, Appl. Catal. B: Environ. 19 (1998) 103–117.
[44] R. Khodayari, C.U.I. Odenbrand, Appl. Catal. B: Environ. 33 (2001) 277–291.
[45] C. Yanxin, J. Yi, L. Wenzhao, J. Rongchao, T. Shaozhen, H. Wenbin, Catal. Today 50 (1999) 39–47.
[46] W. Xu, H. He, Y. Yu, J. Phys. Chem. A 113 (2009) 4426–4432.
[47] M. Waqif, P. Bazin, O. Saur, J.C. Lavalley, G. Blanchard, O. Touret, Appl. Catal. B: Environ. 11 (1997) 193–205.
[48] S. Lucas, E. Champion, D. Bernache-Assollant, G. Leroy, J. Solid State Chem. 177 (2004) 1302–1311.